Hybrid FEA and Meta-modeling for DE Optimization of a PM Stator-excited Motor with a Reluctance Rotor

Oluwaseun A. Badewa, and Dan M. Ionel

SPARK Laboratory, Stanley and Karen Pigman College of Engineering, University of Kentucky, Lexington, KY, USA
o.badewa@uky.edu, dan.ionel@ieee.org

***Abstract*—This paper presents an innovative method for designing high-performance electric motors by integrating machine learning (ML) based meta-modeling with a differential evolution (DE) optimization algorithm. The approach utilizes finite element analysis (FEA) data to train the ML meta-model, allowing for efficient optimization of high-power-density machines, such as the reluctance rotor and permanent magnet (PM) stator combined excitation motor, which is characterized by nonlinearities. The meta-modeling process employs an Artificial Neural Network (ANN) with 3 hidden layers and uses the motor's geometrical variables as inputs. The accuracy of the meta-model in capturing the nonlinear relationships between design parameters, core losses, and torque is assessed using metrics such as R-squared (R^2), normalized root mean square error (NRMSE), and mean absolute percentage error (MAPE), showing promising performance. This hybrid ML-DE framework aims to serve as an alternative approach for physics-based electric motor design and optimization, delivering substantial reductions in computational effort without compromising accuracy. Drive cycle analysis, which could benefit from a system-level optimization integration with the meta-model, was also investigated for a 100kW rated experimentally tested prototype of the studied motor topology with promising results.**

***Index Terms*—Meta-modeling, machine learning, artificial intelligence, differential evolution, finite element analysis, synchronous motor, spoke-type PM, reluctance rotor.**

I. Introduction

The design optimization of electric motors for applications in traction and propulsion is a nonlinear, multi-objective problem that is being researched continuously [1], [2]. With the increasing demand for high-performance, compact designs, system-level optimization is increasingly being proposed to consider not only electromagnetics but also to include mechanical, thermal, and application-specific factors, such as drive cycles [3]–[5]. Therefore, the choice of design optimization strategy and motor topology is central to any application. Several deterministic and stochastic approaches, such as sequential unconstrained minimization techniques (SUMT), Genetic Algorithms (GA), and Differential Evolution (DE), have been adopted to obtain optimal motor designs, given the nonlinearities present in these machines [1], [6]. These methods typically require a large number of candidate designs and lengthy computational times, necessitating research into more computationally efficient methods, for example, surrogate modeling using Kriging techniques [7], [8].

With the rapid developments in artificial intelligence (AI), machine learning (ML), and big data analysis, more feasibility studies are being conducted to explore the potential integration of these technologies with design and optimization workflows [9]–[11]. Meta-models are being developed using neural network architectures, such as Artificial Neural Networks (ANNs) [12], Convolutional Neural Networks (CNNs) [13], and Generative Adversarial Networks (GANs) [14]. They aim to provide an alternative to computationally intensive methods, such as finite element analysis (FEA), by learning nonlinear relationships and subsequently emulating them [8], [15].

Regarding the motor topology, the reluctance rotor and permanent magnet (PM) stator combined excitation motor, which benefits from the flux intensification techniques of spoke-type PMs, especially in its outer rotor configuration, has shown promise for high-speed, high-power-density operation. It also offers additional benefits, including reduced losses due to shortened end turns of the toroidal coils, modular construction, and the potential for advanced stator-only cooling and high slot fill factors using hairpin winding techniques [16], [17]. Given its inherent nonlinearities, this synchronous motor can benefit from accelerated optimization through meta-modeling.

This paper investigates the application of an ANN meta-model, trained with minimal FEA data obtained via DE, to predict performance metrics for inner-rotor PM-stator-excited synchronous motor designs. The proposed approach emulates FEA to enable faster and more efficient design optimization. Unlike traditional ANN training methods that rely on sampling techniques, such as Latin Supercube or Monte Carlo Sampling, this method integrates DE to generate training data. Furthermore, it seeks to optimize the torque-to-stack-length ratio for high-torque-output designs. The subsequent sections of this paper provide a review of the motor topology, discuss the design optimization process, and outline the proposed methodology. The results are evaluated, followed by a discussion on the potential application in the drive cycle analysis of an experimentally validated prototype and conclusions are drawn.

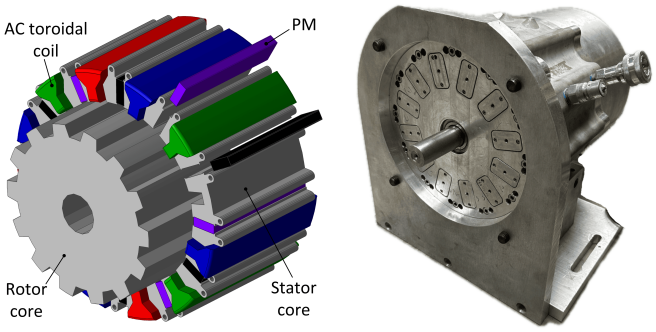

(a) (b)

Fig. 1. The studied inner-rotor permanent magnet (IR-PM) motor topology showing (a) an exploded view of a solid model with concentrated AC coils and spoke-type PMs, and (b) an existing experimentally tested 100kW prototype motor.

II. Operation and Design

The reluctance rotor and PM stator combined excitation motor topology in its inner-rotor configuration (IR-PM), with an example rendering shown in Fig. 1a, and an experimentally validated prototype in Fig. 1b, has a strong nonlinear nature due to saturation effects in its ferrous core. It has been proposed for high-power density applications with several advantages, such as its high airgap flux density capability, modular construction, and reduced losses due to the use of toroidal coils with shortened end turns. Other benefits include simple rotor construction for high-speed operation and the potential for a high slot fill factor using rectangular slots and hairpin winding techniques, as well as integrated advanced stator cooling [17]–[19].

In this machine, with adjacent PMs magnetized in opposite directions, the magnetic flux can be concentrated within the stator, enhancing the effective utilization of the magnets, especially in its outer rotor configuration. The airgap flux density, B_{ag}, can then be obtained as:

$$B_{ag} = B_r \left(\frac{\pi D_g}{4 k_\sigma p h_{PM}} + \frac{2 \mu_r g}{w_{PM}} \right)^{-1}, \qquad (1)$$

where B_r is the PM remanent flux density, D_g is the airgap diameter, k_σ is the leakage coefficient, which can be adjusted to account for the saturation and slotting effect, p is the number of pole pairs, h_{PM} is the PM height along the radius, μ_r is the PM relative permeability, g is the airgap height, and w_{PM} is the PM length in the direction of magnetization.

The electromagnetic torque, T_{emg}, in this synchronous machine, results from the interaction of the dominant airgap flux harmonics from the PMs and armature fields with the rotor reluctance and can be expressed as:

$$T_{emg} = \frac{D_g^2 \ell_{stk}}{4 \mu_0} \int_0^{2\pi} F_{mod}(\theta, t) \Lambda_r(\theta, t) \, d\theta, \qquad (2)$$

where D_g is the airgap diameter, ℓ_{stk} is the stack length, $F_{mod}(\theta, t)$ is the overall modulated MMF, and $\Lambda_r(\theta, t)$ is the rotor permeance function. The interaction between the PM and armature reaction fields with the rotor reluctance results strong nonlinear behavior, which can be observed in the normalized torque and torque constant curves shown in Fig. 3 at very high values of current density.

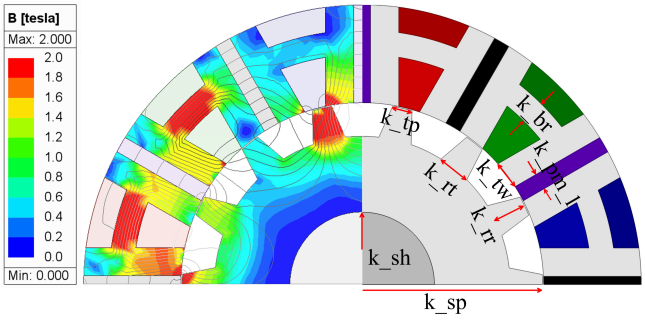

Fig. 2. Cross-sectional view of an IR-PM motor design with 8 labeled geometric independent variables considered in the multi-objective optimization.

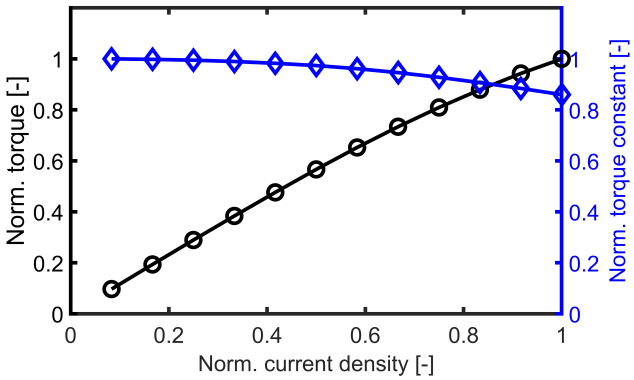

Fig. 3. Torque and torque constant vs. the current density, to show the effect of the nonlinearity as a result of the armature current. Torque and torque constant are normalized based on the peak torque at the maximum current density.

Due to this nonlinearity, exhaustive FEA is required to characterize machine performance comprehensively. This machine may, therefore, benefit from meta-modeling techniques to reduce the computational effort associated with such analyses. In this motor topology, typical polarities are in multiples of 5 and 7. For this study, a 28-pole configuration—resulting from 14 rotor protrusions—is considered for its high power density and efficiency [20], [21].

III. DE and FEA for ML Training

A. Sensitivity analysis

Considering a fixed stator outer diameter of 10″ and an operating speed of 3,000rpm, a 24s28p 2D FEA model was developed for analyses, as shown in Fig. 2. The model has 8 independent geometric variables, as detailed in Table I [22]. A measure of the influence of the geometric variables on motor performance was investigated using a design of experiment (DoE)-based sensitivity analysis. The required FEA parametric models were generated using a central composite design (CCD) method and then analysed using regression and curve fitting techniques to establish a correlation [1], [17], [23].

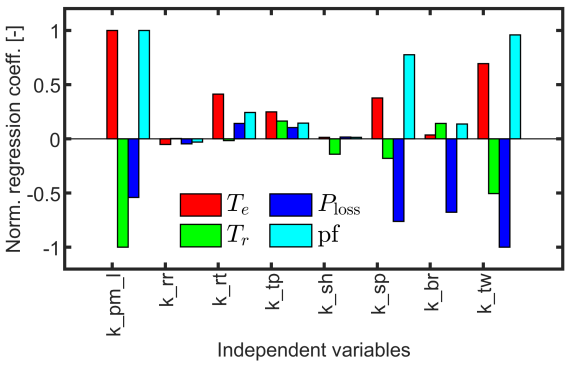

Fig. 4. Normalized nonlinear regression coefficients showing the influence of independent variables at peak loading and expected operating temperature on the average torque, torque ripple, motor loss, and power factor.

Table I
INDEPENDENT VARIABLES FOR THE IR-PM DESIGN OPTIMIZATION, AND THEIR RANGES.

Variable	Description	Min	Max
k_sp	split ratio	0.60	0.70
k_pm_l	PM width ratio	10.00	20.00
k_br	bridge length ratio	0.17	0.33
k_tw	stator tooth width ratio	0.15	0.30
k_sh	shaft dia. ratio	0.30	0.50
k_tp	rotor pole top ratio	0.40	0.80
k_rt	rotor pole root ratio	0.35	0.65
k_rr	rotor pole depth ratio	0.20	0.40

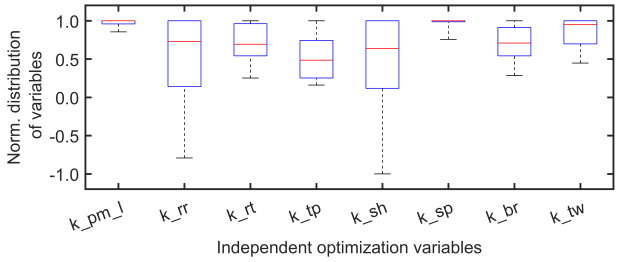

Fig. 5. The distribution of variables for optimal Pareto front designs in the 28-pole IR-PM configuration indicates that a maximum split ratio is preferable, along with thicker PMs oriented in the direction of magnetization, in line with expectations.

For performance indexes of average torque, T_e, torque ripple, T_r, motor loss, P_{loss}, and power factor, pf, and their sensitivity to the independent geometric variables are summarized in Fig. 4. In line with expectations, the PM size influenced torque the most, and the variables related to the active stator determined the motor losses. Since the geometric variables had distributed influences on the studied performance metrics, they were all considered in the DE process for the best result.

B. Differential Evolution (DE)

A 24s28p IR-PM motor parametric model was configured for an outermost diameter of 10″ to optimize for an objective

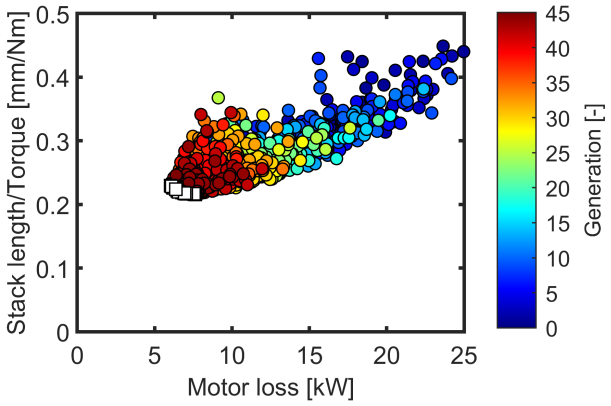

Fig. 6. Optimization results obtained using multi-objective differential evolution for the IR-PM topology for the ratio of stack length to average torque and motor loss objectives. The Pareto designs are shown in white, coming mostly in the last set of generations with a compromise between the two objectives in line with expectations.

electromagnetic torque of 350Nm within the shortest stack length possible using differential evolution (DE). A rated speed of 3,000rpm was considered, which would result in a power output of 100kW, typical for industrial applications [24]–[26]. Multi-objective DE optimization employing FEA was carried out to *minimize* two concurrent objectives relating to the ratio of stack length to average torque, $\mathcal{F}_1$, and motor loss, $\mathcal{F}_2$:

$$\begin{aligned} \mathcal{F}_1 &= \frac{\ell_{stk}}{T_e}, \\ \mathcal{F}_2 &= P_{loss} = P_{Cu} + P_{Fe}, \end{aligned} \tag{3}$$

where ℓ_{stk} is the stack length and T_{avg} is the average value of electromagnetic torque. The objective function for motor loss, P_{loss}, was calculated as the sum of the variable and constant losses of the motor, where P_{Fe} represents the core loss (constant losses) and P_{Cu} represents the copper loss (variable losses) at a current density of 30A/mm^2 with anticipated liquid cooling.

A two-tier analysis is employed to ensure that each design meets the required rated torque of 350Nm at a rated speed of 3,000rpm. Initially, torque is calculated using FEA, and then the stack length, ℓ_{stk}, is adjusted to achieve the specified rated torque before proceeding with the evaluation of set optimization objectives and other performance criteria. To enhance computational efficiency, the optimization was stopped when a preset number of generations had been solved or there was minimal change of less than 1% in the performance of designs in successive generations. To check that optimal ranges had been correctly set for the independent variables, box plots displaying their distribution for the Pareto designs were examined, as shown in Fig. 5. In line with expectations, thicker magnets in the direction of magnetization are favored for torque maximization, and the maximum split ratio is preferable for loss reduction.

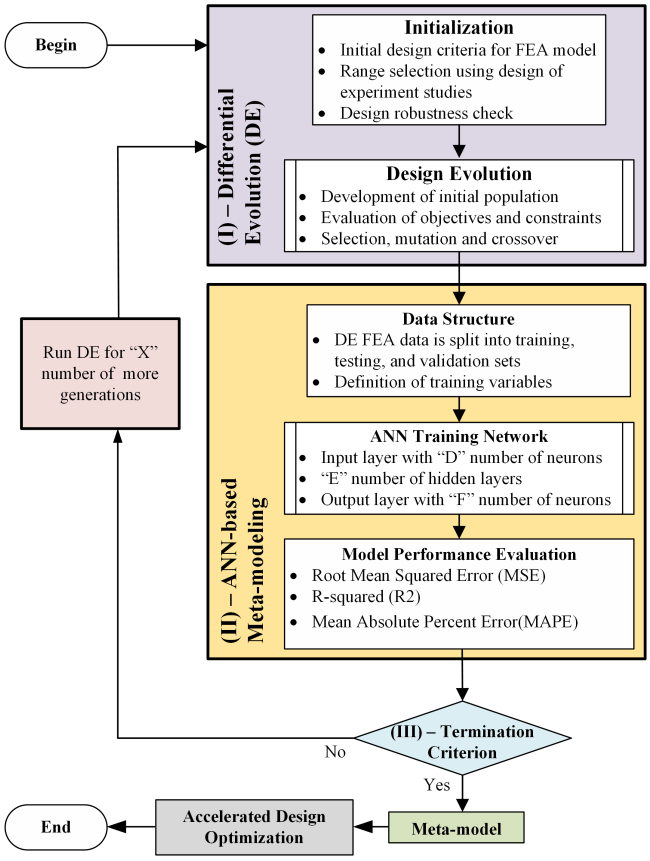

Fig. 7. A flowchart showing the stages in the implemented ANN-based meta-modeling employing differential evolution as an input stage, where D, E, F, and X are integer parameters. A termination criterion based on set test metrics checks training satisfaction, and afterward, a resultant meta-model can be obtained.

IV. Meta-modeling using ANN

Given the nonlinear relationships between geometry and performance in the IR-PM motor, developing a meta-model trained on performance results from FEA of designs generated by DE optimization could provide insights into the feasibility of performance estimation through meta-modeling, offering the potential benefit of reduced computational effort. Using TensorFlow [27], ANN meta-models were developed and trained using the results of DE to predict the ratio, T_e/ℓ_{stk}, and P_{Fe} for IR-PM machine designs. The implemented ANN architecture consists of an input layer, three hidden layers with 128, 64, and 32 neurons, respectively, and a single output layer with one neuron. The novel approach is implemented in the design process, as shown in Fig. 7, with the DE stage serving as an input to the ANN-based meta-modeling stage. The developed meta-model is evaluated after each successive DE generation, and a termination criterion is proposed to check if it is satisfactory. This stopping criteria could include user-defined error values, elapsed computation time, the number of DE generations, or a combination of these factors.

Two ANN models were trained on a dataset of 2,000 candidate designs generated through 2D FEA-based DE optimization (Fig. 6). The ANN model for predicting the ratio

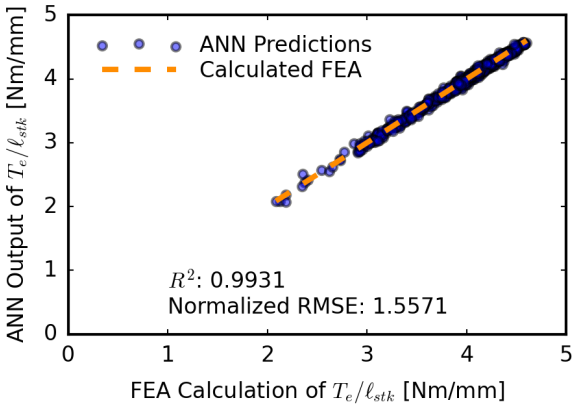

(a)

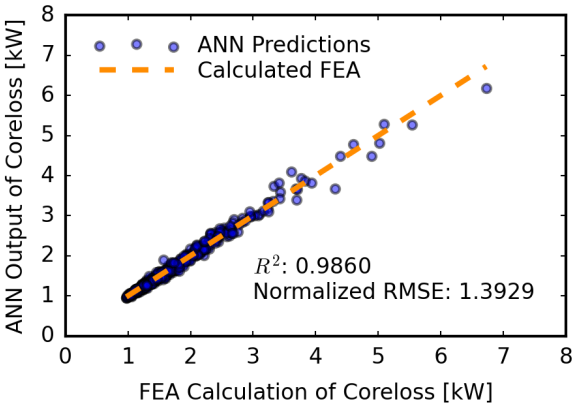

(b)

Fig. 8. The output trends for the ANN-based meta-modeling showing good correlation between the calculated FEA results and ANN predictions for (a) T_e/ℓ_{stk}, and (b) P_{Fe}, with the resulting R^2 and normalized RMSE values indicating high accuracy.

T_e/ℓ_{stk} was trained using 8 geometric input parameters described in Fig. 2, while the model for P_{Fe} included these same parameters along with the stack length, totaling 9 input variables. Since a fixed current density is considered and the geometries of the coils are known, P_{Cu} can be computed mathematically and need not be trained for. From the candidate designs, a random selection of 50% was employed for training, 30% for validation, and the remaining 20% for testing the ANN meta-model. The generalization capability of the ANN will be assessed by analyzing the error values for the training and validation datasets over 50 epochs.

V. Results and Discussion

The performance of the ANN meta-models was evaluated using R-squared (R^2), normalized root mean square error (NRMSE), and mean absolute percentage error (MAPE) metrics. The torque-to-stack-length ratio model, T_e/ℓ_{stk}, achieved an R^2 value of 0.9931, showcasing a strong correspondence between the ANN predictions and FEA outputs, as depicted in Fig. 8a. The NRMSE of 1.56% and MAPE of 0.80% further

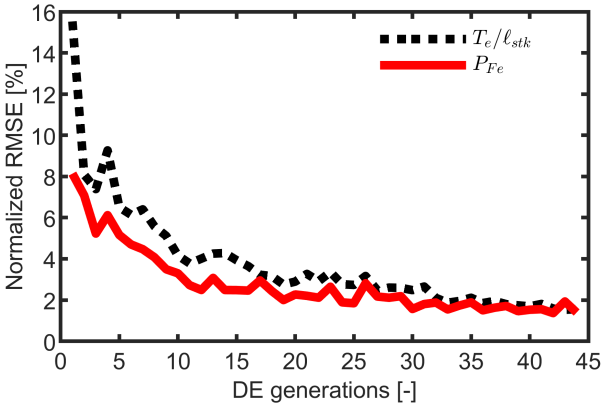

Fig. 9. The progression of normalized RMSE with increasing DE generational data shows a decrease in the error with more training.

Table II
IR-PM PROTOTYPE DRIVE CYCLE ANALYSIS FOR ORANGE COUNTY TRANSIT ASSOCIATION (31 MINUTES) REPORTING THE CENTROIDS AND THEIR CORRESPONDING ENERGY WEIGHTS (C.E.W)

Drive shaft			Motor shaft (assuming a gear ratio)			
Cent. no.	Torque [Nm]	Speed [rpm]	Torque [Nm]	Speed [rpm]	C.E.W [-]	Motor eff. [%]
1	1291	429	215	2575	0.208	91.8
2	946	560	158	3363	0.192	94.0
3	609	648	102	3888	0.190	91.8
4	351	743	59	4461	0.160	86.1
5	1783	442	297	2650	0.157	89.1
6	104	955	17	5730	0.090	74.7
7	87	88	14	530	0.001	88.5

confirm the model's high accuracy in estimating the torque-to-stack-length ratio across different designs. For the core loss model, P_{Fe}, with results shown in Fig. 8b, an R^2 value of 0.9860 indicates a robust correlation between ANN predictions and FEA results. The low NRMSE of 1.39% demonstrates the precision of the model, while an MAPE of 2.61% highlights its minimal deviation from the calculated values.

The error reduction during training, illustrated in Fig. 9, underscores the robustness of the ANN models. Both models exhibit a rapid decrease in NRMSE within the first 10 generations of the differential evolution (DE) optimization process, reflecting their ability to learn complex, nonlinear patterns in the dataset. This suggests the meta-model can replace the FEA in the design optimization after, for example, the 20th generation with NRMSE of about 2%, potentially reducing computational effort by half. The low error metrics and accurate predictions validate the ANN models' ability to capture the nonlinear relationships in T_e/ℓ_{stk} and P_{Fe}. This confirms their effectiveness as meta-models for electromagnetic design tasks, offering a computationally efficient approach that significantly reduces computational costs while maintaining high accuracy.

VI. EXPERIMENTATION AND DRIVE CYCLE ANALYSIS

The feasibility of using meta-modeling to achieve optimal designs for the investigated topology would facilitate the development of prototypes and allow for system-level optimization studies, which could include drive cycle analysis [28], [29]. A 100 kW-rated prototype of the IR-PM topology has been constructed, as shown in Fig. 1b, and experimentally tested at expected high operating temperatures. The resultant efficiency map is shown in Fig. 10, demonstrating the possibility of high-efficiency operation.

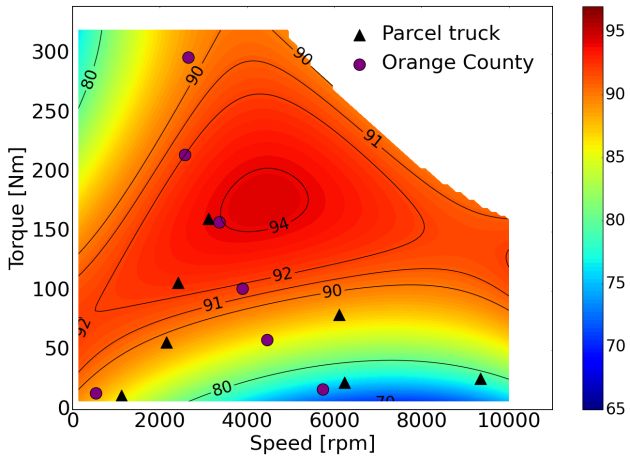

Fig. 10. Measured efficiency map of the prototype machine at high operating temperature showing capability for high-efficiency operation at the most representative points for the NREL Parcel Truck (Baltimore) and Orange County drive cycles.

Considering traction applications in EVs, the prototype was analyzed for two example drive cycles: the NREL Parcel Truck (Baltimore) and Orange County drive cycles [30]. Using the k-means clustering algorithm, the seven most representative points of the cycles (centroids) were obtained, and the performance of the prototype was analyzed at these points, as detailed in Table II and Fig. 10. Following this analysis, efficiency values of 94.1% and 96.8% were obtained for the NREL Parcel Truck and Orange County drive cycles, respectively. Analysis of this nature and the resulting outcomes may be further improved through system-level optimization using meta-model-based optimization.

VII. CONCLUSION

This study explores the feasibility of using ANN meta-models—trained with limited data from differential evolution (DE)—to predict performance metrics in high-power-density cored machine designs. The novel approach was successfully demonstrated on a recently developed nonlinear inner-rotor PM-stator combined-excitation motor topology—a new type of machine for which analytical and well-established design methods are not yet available—offering an efficient alternative to traditional FEA and highlighting Machine Learning (ML) as a significant path forward in its development. Furthermore, these meta-models may enable accelerated large-scale system-level optimization, such as drive cycle analysis, thereby enhancing the overall design and evaluation process of such advanced motor topologies.

The ANN meta-models for torque-to-stack-length ratio (T_e/ℓ_{stk}) and core loss (P_{Fe}) demonstrated high accuracy, with R^2 values of 0.9931 and 0.9860, and NRMSEs of 1.56% and 1.39%, respectively. Their NRMSE dropped to about 2% by the 20th DE generation, at which point the FEA could be replaced, saving up to half of the computational time. The ANN models' low error values and robust predictions indicate their potential as computationally efficient surrogates for design optimization.

ACKNOWLEDGMENT

The support of QM Power Inc. for the development of the prototype, of Ansys Inc. for the FEA software, and of University of Kentucky, the L. Stanley Pigman Chair in Power Endowment for publication is gratefully acknowledged.

REFERENCES

[1] M. Rosu, P. Zhou, D. Lin, D. M. Ionel, M. Popescu, F. Blaabjerg, V. Rallabandi, and D. Staton, *Multiphysics simulation by design for electrical machines, power electronics and drives*. John Wiley & Sons, 2017.

[2] I. Boldea, L. N. Tutelea, and A. A. Popa, "Reluctance synchronous and flux-modulation machines designs: Recent progress," *IEEE Journal of Emerging and Selected Topics in Power Electronics*, vol. 10, no. 2, pp. 1683–1702, 2022.

[3] M. Popescu, L. Di Leonardo, G. Fabri, G. Volpe, N. Riviere, and M. Villani, "Design of induction motors with flat wires and copper rotor for E-Vehicles traction system," *IEEE Transactions on Industry Applications*, vol. 59, no. 3, pp. 3889–3900, 2023.

[4] S. Pastellides, S. Gerber, R.-J. Wang, and M. Kamper, "Evaluation of drive cycle-based traction motor design strategies using gradient optimisation," *Energies*, vol. 15, no. 3, p. 1095, 2022.

[5] M. Helbing, S. Uebel, C. Matthes, and B. Bäker, "Comparative case study of a metamodel-based electric vehicle powertrain design," *IEEE Access*, vol. 9, pp. 160 823–160 835, 2021.

[6] M. Abdalmagid, E. Sayed, M. H. Bakr, and A. Emadi, "Geometry and topology optimization of switched reluctance machines: A review," *IEEE Access*, vol. 10, pp. 5141–5170, 2022.

[7] N. Taran, D. M. Ionel, and D. G. Dorrell, "Two-level surrogate-assisted differential evolution multi-objective optimization of electric machines using 3-D FEA," *IEEE Transactions on Magnetics*, vol. 54, no. 11, pp. 1–5, 2018.

[8] M. Cheng, X. Zhao, M. Dhimish, W. Qiu, and S. Niu, "A review of data-driven surrogate models for design optimization of electric motors," *IEEE Transactions on Transportation Electrification*, pp. 1–1, 2024.

[9] Y. Li, G. Lei, G. Bramerdorfer, S. Peng, X. Sun, and J. Zhu, "Machine learning for design optimization of electromagnetic devices: Recent developments and future directions," *Applied Sciences*, vol. 11, no. 4, 2021. [Online]. Available: https://www.mdpi.com/2076-3417/11/4/1627

[10] M. Omar, M. Bakr, and A. Emadi, "Switched reluctance motor design optimization: A framework for effective machine learning algorithm selection and evaluation," in *2024 IEEE Transportation Electrification Conference and Expo (ITEC)*, 2024, pp. 1–6.

[11] V. Parekh, D. Flore, and S. Schöps, "Deep learning-based meta-modeling for multi-objective technology optimization of electrical machines," *IEEE Access*, vol. 11, pp. 93 420–93 430, 2023.

[12] A.-C. Pop, Z. Cai, and J. J. C. Gyselinck, "Machine-learning aided multiobjective optimization of electric machines— geometric-feasibility and enhanced regression models," *IEEE Journal of Emerging and Selected Topics in Industrial Electronics*, vol. 4, no. 3, pp. 844–854, 2023.

[13] H. Sasaki, Y. Hidaka, and H. Igarashi, "Prediction of IPM machine torque characteristics using deep learning based on magnetic field distribution," *IEEE Access*, vol. 10, pp. 60 814–60 822, 2022.

[14] H. Wu, S. Niu, Y. Zhang, X. Zhao, and W. Fu, "Fast magnetic field approximation method for simulation of coaxial magnetic gears using AI," *IEEE Journal of Emerging and Selected Topics in Industrial Electronics*, vol. 4, no. 1, pp. 400–408, 2023.

[15] C. He, Y. Zhang, D. Gong, and X. Ji, "A review of surrogate-assisted evolutionary algorithms for expensive optimization problems," *Expert Systems with Applications*, vol. 217, p. 119495, 2023.

[16] C. S. Goli, M. G. Kesgin, P. Han, D. M. Ionel, S. Essakiappan, J. Gafford, and M. D. Manjrekar, "Analysis and design of an electric machine employing a special stator with phase winding modules and PMs and a reluctance rotor," *IEEE Access*, vol. 12, pp. 9621–9631, 2024.

[17] O. A. Badewa and D. M. Ionel, "Comparative analysis of motors with inner and outer reluctance rotors and PM stators," in *2024 IEEE Transportation Electrification Conference and Expo (ITEC)*, 2024, pp. 1–6.

[18] A. Kampker, H. H. Heimes, B. Dorn, F. Brans, and C. Stäck, "Challenges of the continuous hairpin technology for production techniques," *Energy Reports*, vol. 9, pp. 107–114, 2023.

[19] S. Paul, J.-G. Lee, P.-W. Han, J. Chang, and X.-T. Luong, "Design consideration of rectangular conductors and slot wedge for AC winding loss reduction in high speed train traction motor," *IEEE Transactions on Vehicular Technology*, vol. 73, no. 11, pp. 16 543–16 556, 2024.

[20] O. A. Badewa, A. Mohammadi, D. D. Lewis, D. M. Ionel, S. Essakiappan, and M. Manjrekar, "Optimization of an electric vehicle traction motor with a PM flux intensifying stator and a reluctance outer rotor," in *2023 IEEE Transportation Electrification Conference & Expo (ITEC)*, 2023, pp. 1–6.

[21] O. A. Badewa, A. Mohammadi, D. D. Lewis, S. Essakiappan, M. Manjrekar, and D. M. Ionel, "Electromagnetic design characterization of synchronous machines with flux switching effect employing reluctance rotors and stators with PMs and AC concentrated coils," *IEEE Transactions on Industry Applications*, pp. 1–14, 2025.

[22] *Ansys® Electronics, version 24.1, 2024, ANSYS Inc.*

[23] P. Asef and A. Lapthorn, "Overview of sensitivity analysis methods capabilities for traction AC machines in electrified vehicles," *IEEE Access*, vol. 9, pp. 23 454–23 471, 2021.

[24] I. Boldea, I. Torac, and L. Tutelea, "100kW 6-12krpm ALA rotor traction motor: preliminary design with key electromagnetic FEM validation," in *IEEE EUROCON 2023 - 20th International Conference on Smart Technologies*, 2023, pp. 602–607.

[25] N. Tang and I. P. Brown, "Comparison of candidate designs and performance optimization for an electric traction motor targeting 50 kW/L power density," in *2021 IEEE Energy Conversion Congress and Exposition (ECCE)*, 2021, pp. 3675–3682.

[26] P. Asef and C. Vagg, "A physics-informed bayesian optimization method for rapid development of electrical machines," *Scientific Reports*, vol. 14, no. 1, p. 4526, 2024.

[27] M. Abadi *et al.*, "TensorFlow: Large-scale machine learning on heterogeneous systems," 2015, software available from tensorflow.org. [Online]. Available: https://www.tensorflow.org/

[28] O. Borsboom, M. Salazar, and T. Hofman, "Design optimization of electric vehicle drivetrains using surrogate modeling frameworks," *Authorea Preprints*, 2025.

[29] M. Gobbi, A. Sattar, R. Palazzetti, and G. Mastinu, "Traction motors for electric vehicles: Maximization of mechanical efficiency–a review," *Applied Energy*, vol. 357, p. 122496, 2024.

[30] Drivecat: Drive cycle analysis tool. [Online]. Available: https://www.nrel.gov/transportation/drive-cycle-tool/